AFCRL-66-586

"Implementation and Performance of the Maximum-Likelihood Detector in a Channel with Intersymbol Interference"

by

Robert A. Gonsalves

Northeastern University
360 Huntington Avenue
Boston, Massachusetts

Contract No. AF19(628)-3312

Project No. 4610

Task No. 461003

Scientific Report No. 5

August 1966

Charles F. Hobbs, CRBK

This research was supported in part by the National Aeronautics and Space Administration under Grant NGR-22-011-013 (ERC, Cambridge, Massachusetts)

Prepared

for

AIR FORCE CAMBRIDGE RESEARCH LABORATORIES
OFFICE OF AEROSPACE RESEARCH
UNITED STATES AIR FORCE
BEDFORD, MASSACHUSETTS

AFCRL-66-586

"Implementation and Performance of the Maximum-Likelihood Detector in a Channel with Intersymbol Interference"

by

Robert A. Gonsalves

Northeastern University
360 Huntington Avenue
Boston, Massachusetts

Contract No. AF19(628)-3312

Project No. 4610

Task No. 461003

Scientific Report No. 5

August 1966

Charles F. Hobbs, CRBK

This research was supported in part by the National Aeronautics and Space Administration under Grant NGR-22-011-013 (ERC, Cambridge, Massachusetts)

Prepared

for

AIR FORCE CAMBRIDGE RESEARCH LABORATORIES
OFFICE OF AEROSPACE RESEARCH
UNITED STATES AIR FORCE
BEDFORD, MASSACHUSETTS

ACKNOWLEDGEMENT

Arthur A. Giordano helped to establish the second piece-wise linear approximation of Section III and Eric Reid programmed Equation (28) to provide the graphs of Figures 6 through 9.

ABSTRACT

It is shown that the maximum-likelihood (ML) detector for noisy, binary channel with restricted intersymbol interference (ISI) consists of a matched filter followed by a tapped delay line. The useful output is a nonlinear function of the tap outputs. Bounds on the per-symbol probability of error indicate that a gross approximation to the ML detector performs as well as an optimum linear detector. The major assumptions are (1) bi-polar binary signals, (2) ISI only between adjacent bauds, (3) stationary additive white, Gaussian noise, and (4) perfect synchronization. Extensions are suggested to remove assumptions (1) and (2) and to handle stationary, non-white Gaussian noise.

TABLE OF CONTENTS

LIST OF FIGURES

1. Introduction

In a previous report[1] it was shown that the maximum-likelihood (ML) detector for a noisy, binary channel with memory could be implemented using two matched filters, one delay element and a recorder-play-back system. In this report we will modify and streamline the detector structure so that it includes only one matched filter and so that decisions can be made sequentially, in real time. We find new upper and lower bounds for the detector's performance by certain limiting techniques. We also discuss some extensions to the earlier work.

There are four key assumptions for the main body of this report:

(1) The signal is

$$\sum_{n=-\infty}^{\infty} \mu_k \, s(t-kT),$$

where $\mu_k = +1$ or -1, represents the k^{th} symbol to be transmitted. The μ_k's are independent and $s(t)$ is known exactly. Thus we focus our attention on the binary detection of a known signal. In Section 5 we discuss briefly the multi-level case. If $s(t)$ is not known exactly, then we assume that it can be suitably measured during a brief calibration run or can be determined, adaptively, during transmission.

(2) The signal $s(t)$ is smeared only into one adjacent baud. Thus $s(t)$ lasts only from 0 to 2T. This restriction is also examined in Section 5.

(3) The noise is white, additive and Gaussian. Colored noise can be handled by suitable pre-whitening[2] prior to detection. In that case s(t) would be the output of the pre-whitening filter and would be subject to restriction (2) on page 1.

(4) Synchronism is maintained between transmitter and receiver. This may be achieved, for example, by the transmission of recurrent synch pulses.

The ML detector discussed in this report is new in two respects. First of all, although it has the general appearance of the linear, tapped-delay line detectors offered by Lucky[3] and by others[4,5], it has been developed without the constraint of linearity. Thus the ML detector will always yield a probability of error that is smaller than the corresponding linear detector (except in some limiting cases where the performances will be identical). In this sense the ML detector is mathematically equivalent to that derived in the earlier report[1], the implementation is different and is, in fact, inspired by the linear detectors of Lucky[3] and Tufts.[5]

Finally, the new detector structure suggests a piece-wise linear approximation to the optimum detector, which is quite simple to implement. The approximation is an extension to the class of "feedback tail cancellation" schemes discussed by Tufts and others (see Tufts[5] and the "switched mode" detector of Aein and Hancock[6]). Because of its simplicity and near optimum performance, it merits consideration in an actual binary transmission system.

2. The Detector Specification and Structure

In [1] we show that the ML detector first computes

$$A_k = \frac{4}{N_o} \int_{kT}^{(k+2)T} y(t)\, s(t-kT)\, dt, \tag{1}$$

where $y(t)$ is the received signal,

$$y(t) = \sum_{k=-\infty}^{\infty} \mu_k\, s(t-kT) + n(t), \tag{2}$$

and $n(t)$ is the additive, white, Gaussian noise of double-sided power spectral density $N_o/2$ watts per cps. A_k represents the correlation of the signal $(+)s(t-kT)$ with the received signal and can be implemented with a matched filter or with a multiplier and integrator.

The detector then bases its decision about the polarity of μ_k on the statistic Λ_k [1],

$$\Lambda_k = A_k + Z\{A_{k-1} + Z\{A_{k-2} + \cdots\}\} + Z\{A_{k+1} + Z\{A_{k+2} + \cdots\}\}, \tag{3}$$

where

$$Z\{x\} \equiv \log_e \frac{e^x + e^R}{1 + e^{x+R}} \tag{4}$$

and

$$R \equiv \frac{4}{N_o} \int_0^{2T} s(t)\, s(t+T)\, dt. \tag{5}$$

For example, if the source probabilities are equal and the costs associated with each type of error are equal, then the detector decides

$$\mu_k = \begin{cases} 1 & \text{if } \Lambda_k > 0 \\ -1 & \text{if } \Lambda_k < 0 \end{cases} .$$

Note that we may express R as

$$R = 2\rho r \tag{6}$$

where ρ, defined as

$$\rho \equiv \frac{\int_0^{2T} s^2(t)\, dt}{\frac{N_o}{2}} , \tag{7}$$

is the signal-to-noise ratio and r, defined as

$$r \equiv \frac{\int_0^{2T} s(t)\, s(t+T)\, dt}{\int_0^{2T} s^2(t)\, dt} , \tag{8}$$

will be called the index of interference and is a measure of the harmful effects of intersymbol interference. Now r is loosely bounded by

$$-1 < r < 1$$

so we expect that in the face of severe interference R will have values of the same order of magnitude as ρ.

Equations (2) and (3) define the ML detector and the corresponding structure is shown in Fig. 1. Note the similarity between this structure and those of Lucky[3] and of Tufts[4], that is, a matched filter followed by a tapped delay line. In this structure, however, the useful output is mot merely a weighted sum of the tap outputs. Here each output is added to its neighbor after that neighbor is passed through a non-linear amplifier (the box labelled Z and defined by Equation (4)). The M taps to the left of the center tap, the useful output, indicate that M bauds of the past data have been optimally processed to aid in the decision on μ_k. The N taps to the right indicate that N future bauds have also been considered. In theory one should let $M \to \infty$ and $N \to \infty$ to achieve the optimum detector structure. We can, in fact, achieve $M \to \infty$, that is, we can consider all past data, by a modification of Fig. 1. This modification is shown in Fig. 2. Obviously, a consideration of all future data required infinite delay (for an infinite binary sequence) so a finite N must be chosen based on a study of cost per additional section versus improved performance per additional section (assuming the associated increased delay is acceptable). Such a study is very difficult analytically and is probably best done experimentally.

One of the interesting features of the detector structure of Fig. 2 is that all the non-linear amplifiers, the Z boxes, are identical. Therefore, knowing the signal shape s(t) (so that the matched filter can be constructed), the detector structure is determined by a specification of the parameter R as given by (5) or (6), since the amplifier characteristics depend only on R. In Fig. 3 we show the Z-box amplifier input-output characteristics for several typical values of R. Note that these curves are fairly well behaved and saturate at $\pm R$.

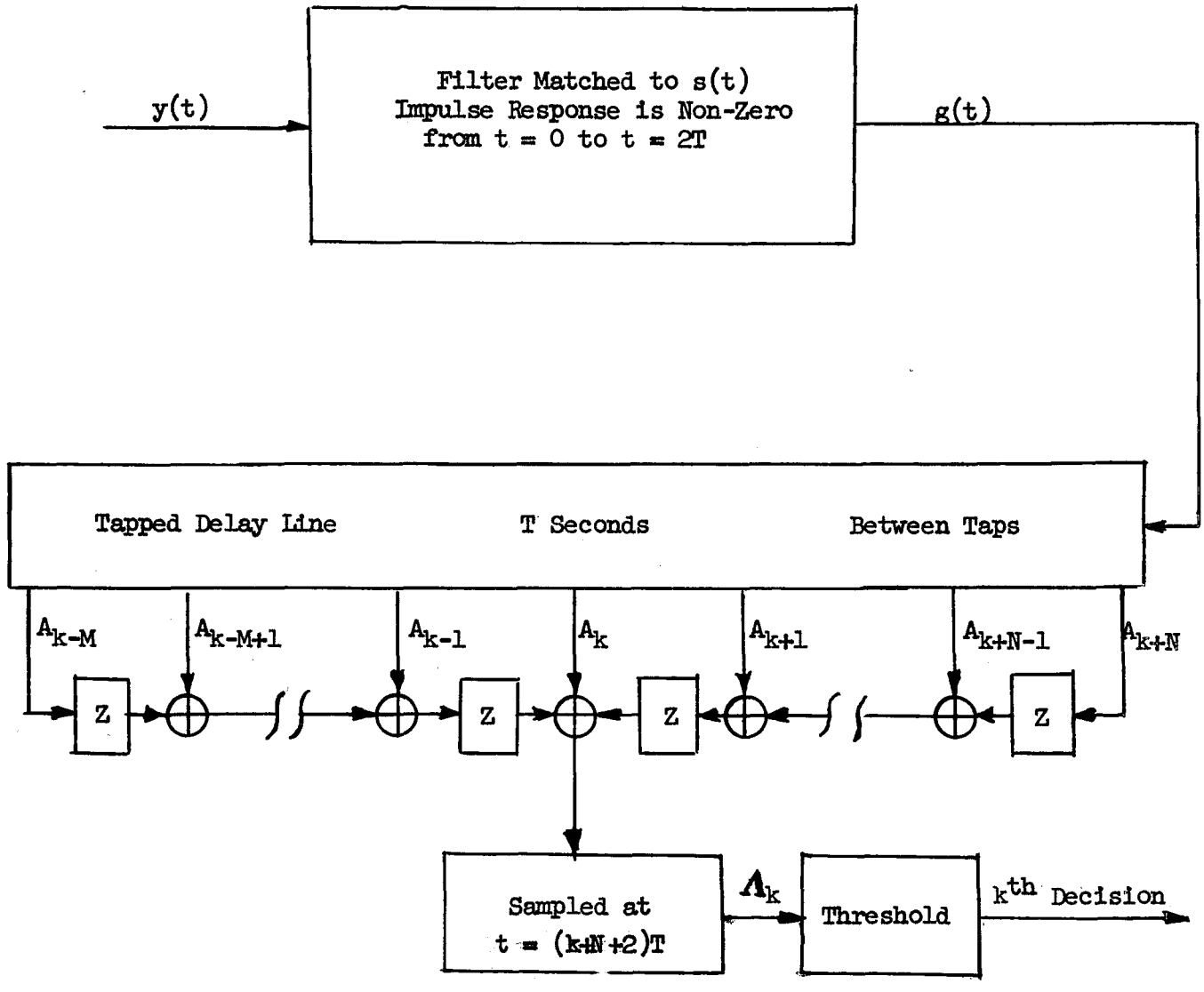

Fig. 1 The ML Receiver

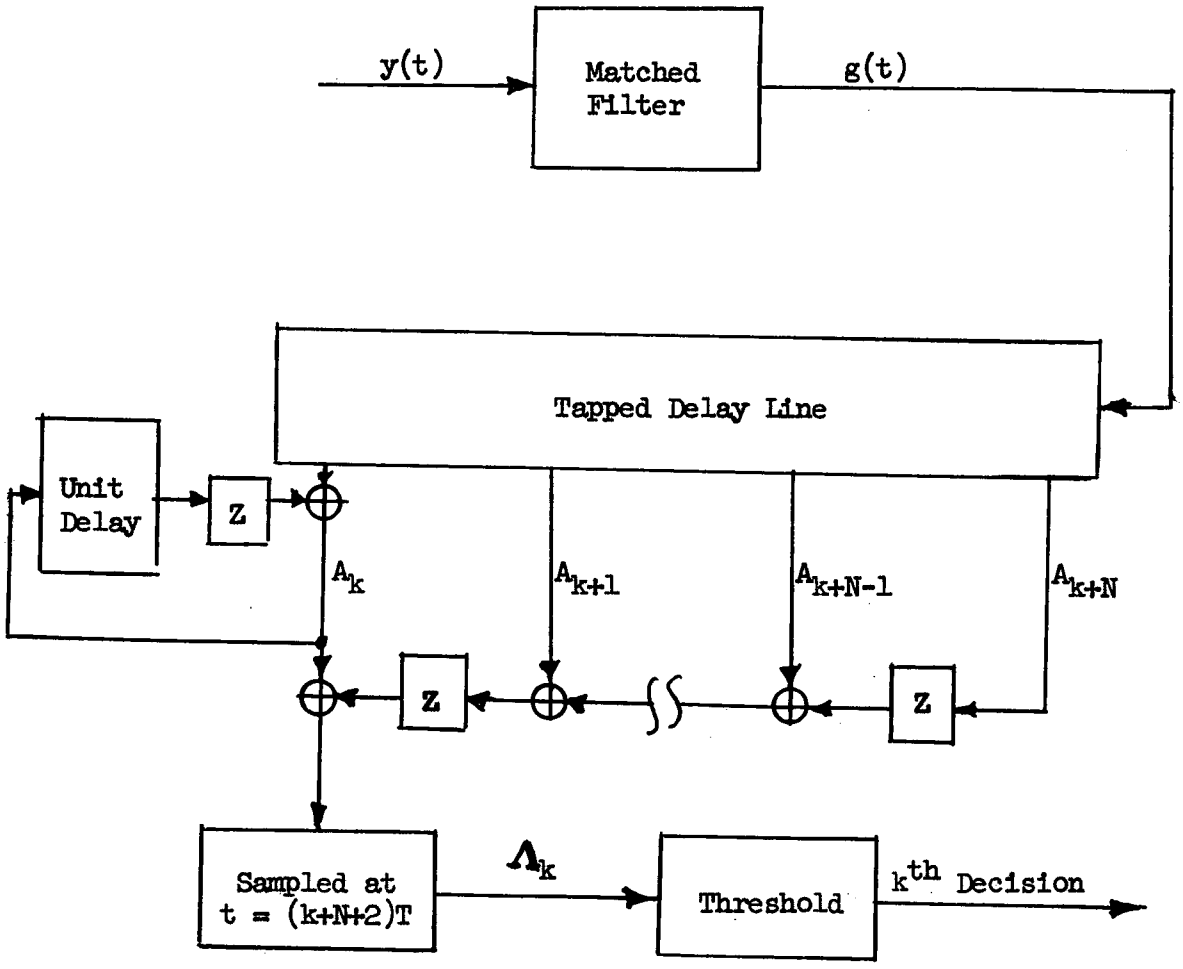

Fig. 2 A Simplified ML Receiver

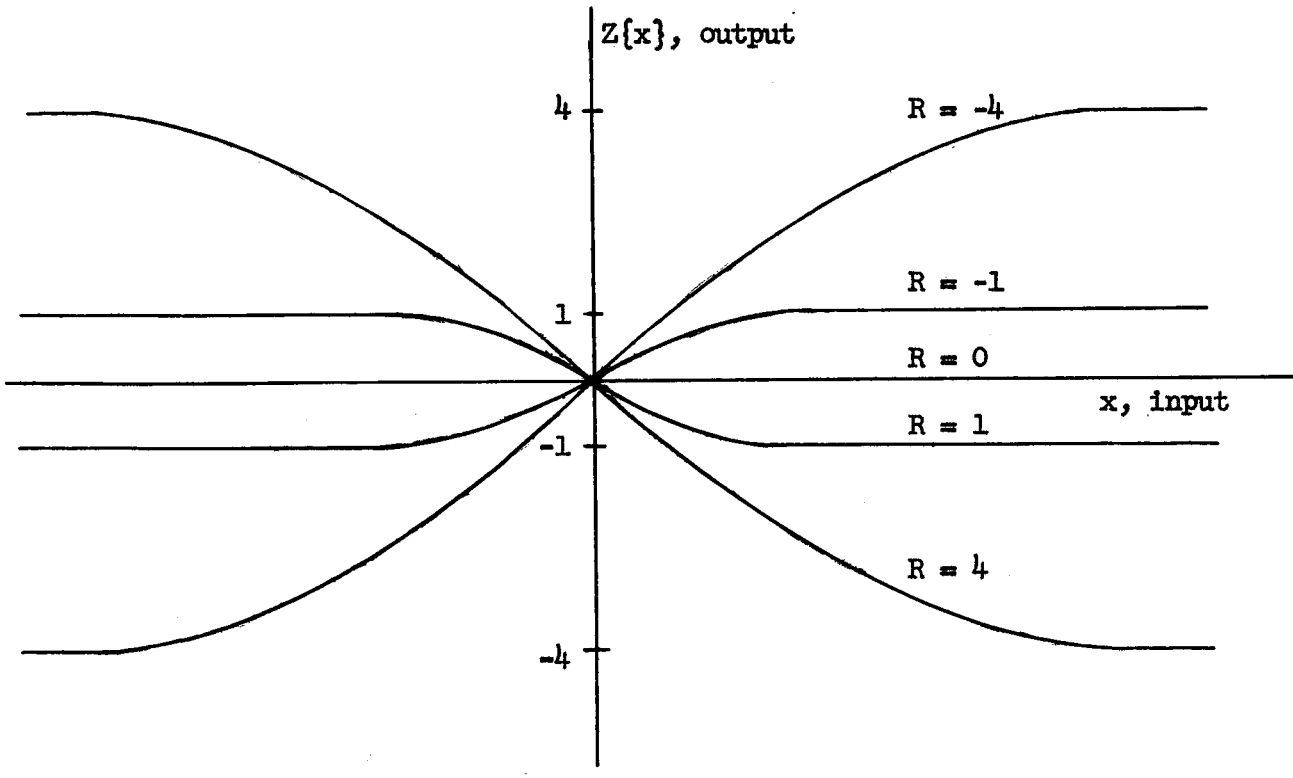

Fig. 3 The Non-Linear Amplifier, Z{x}

To provide insight into the detector operation let us assume that the detector of Fig. 2 uses no tapped delay line at all. Hence

$$\Lambda_k = A_k + Z\{A_{k-1} + Z\{A_{k+2} + \cdots\}\}.$$

We see that the k^{th} decision statistic contains first of all the correlation of $s(t-kT)$ with the received signal, namely A_k. The other additive term is bounded by $\pm R$. In fact, assuming high SNR, A_{k-1} will be either large positive for $\mu_{k-1} = 1$ or large negative for $\mu_{k-1} = -1$. Thus referring to Fig. 3, we will subtract R from A_k if μ_{k-1} is positive and we will add R to A_k if μ_{k-1} is negative. This addition or subtraction of R is mathematically equivalent to subtracting out the channel memory and is, therefore, a "feedback tail cancellation" scheme as mentioned in the introduction. The novelty here is that the tail cancellation occurs on a probabilistic basis. That is, we do not simply allow R or -R but we choose an intermediate value based on $A_{k-1} + Z\{A_{k-2} + \cdots\}$, which is a measure of our certainty concerning μ_{k-1}.

To examine the effect of the future data on the detector, we may consider that the data has been received with time reversed. Thus the "tail" of the original pulse becomes the main body of the new pulse and vice-versa. We can perform a similar, probabilistic tail cancellation. One then combines the information concerning past and future in the center tap to obtain the ML statistic.

3. Piece-Wise Linear Approximations

Two, successively better approximations to the ML detector are considered. Both are really approximations on the function $Z\{x\}$ so that the block diagram specification of Fig. 2 is still applicable.

The first approximation is $Z'\{x\}$,

$$Z'\{x\} \equiv -R\ \mathrm{Sgn}\{x\} \tag{9}$$

where

$$\mathrm{Sgn}\{x\} \equiv \begin{cases} 1, & x > 0 \\ -1, & x < 0\ . \end{cases}$$

If one considers only past data, then the resulting detector is exactly a tail cancellation scheme as previously discussed. Consideration of future data, as is done in Fig. 2, represents an improvement over previous detectors of this type. The performance of this detector, with a slight modification, is considered in the next section and serves as the upper bound on the ML detector.

A good approximation $Z''\{x\}$ to $Z\{x\}$ is shown in Fig. 4. In that figure the attenuator, A, is given by

$$A = \frac{|R/2|}{\ell n\ \dfrac{e^{|R|} - e^{-|R/2|}}{e^{|R/2|} - 1}} \tag{10}$$

This choice of A, together with the subsequent piece-wise linear amplifier z, yields an approximation that is exact for very small and for very large values of x and also for those x for which $Z\{x\} = \pm R/2$. This second approximation is especially good for large $R(R > 16)$ as can be seen from Fig. 5 where $\frac{1}{R} Z\{x\}$ is plotted versus $\frac{Ax}{R}$ for several values of R.

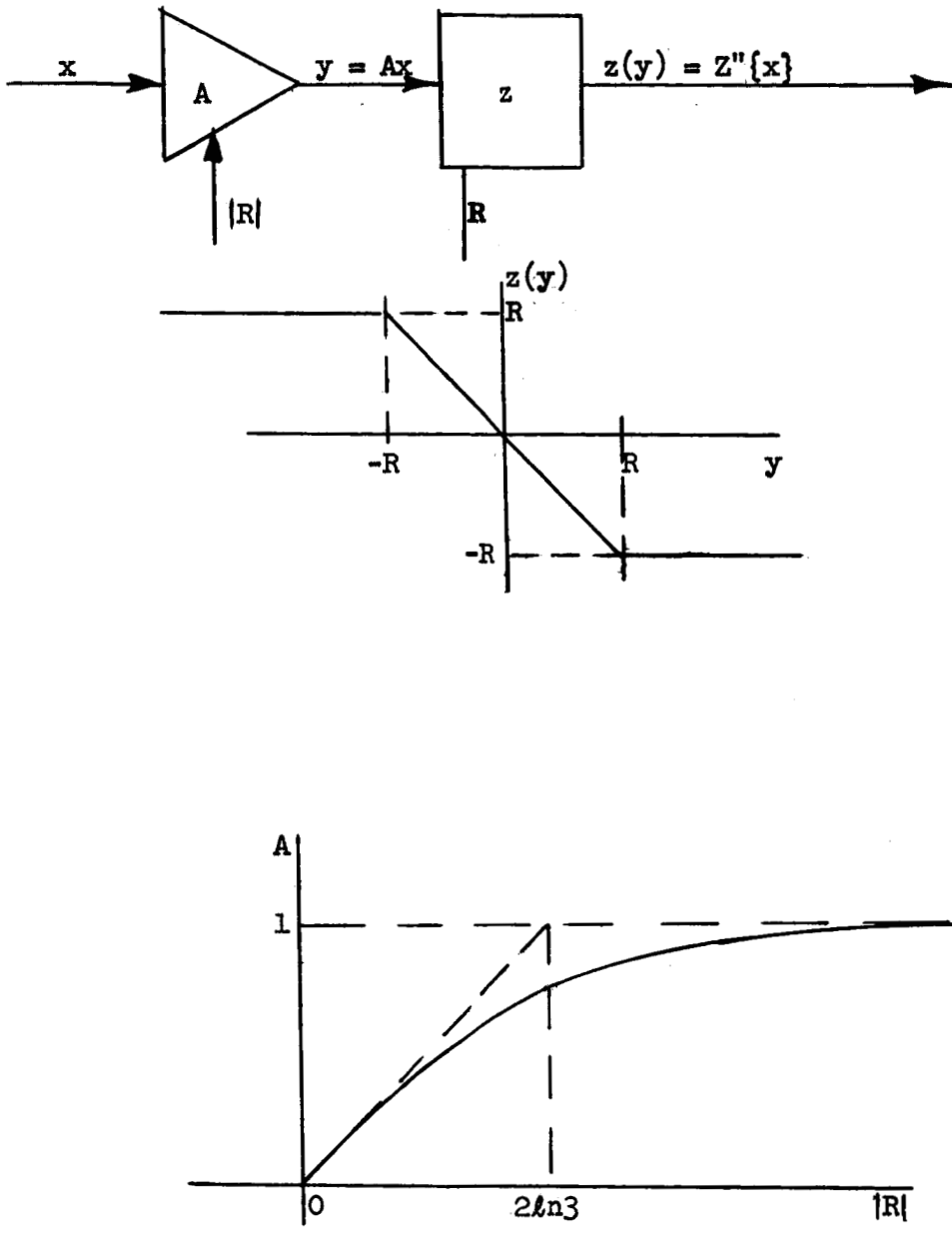

Fig. 4 Second Approximation to Z{x}

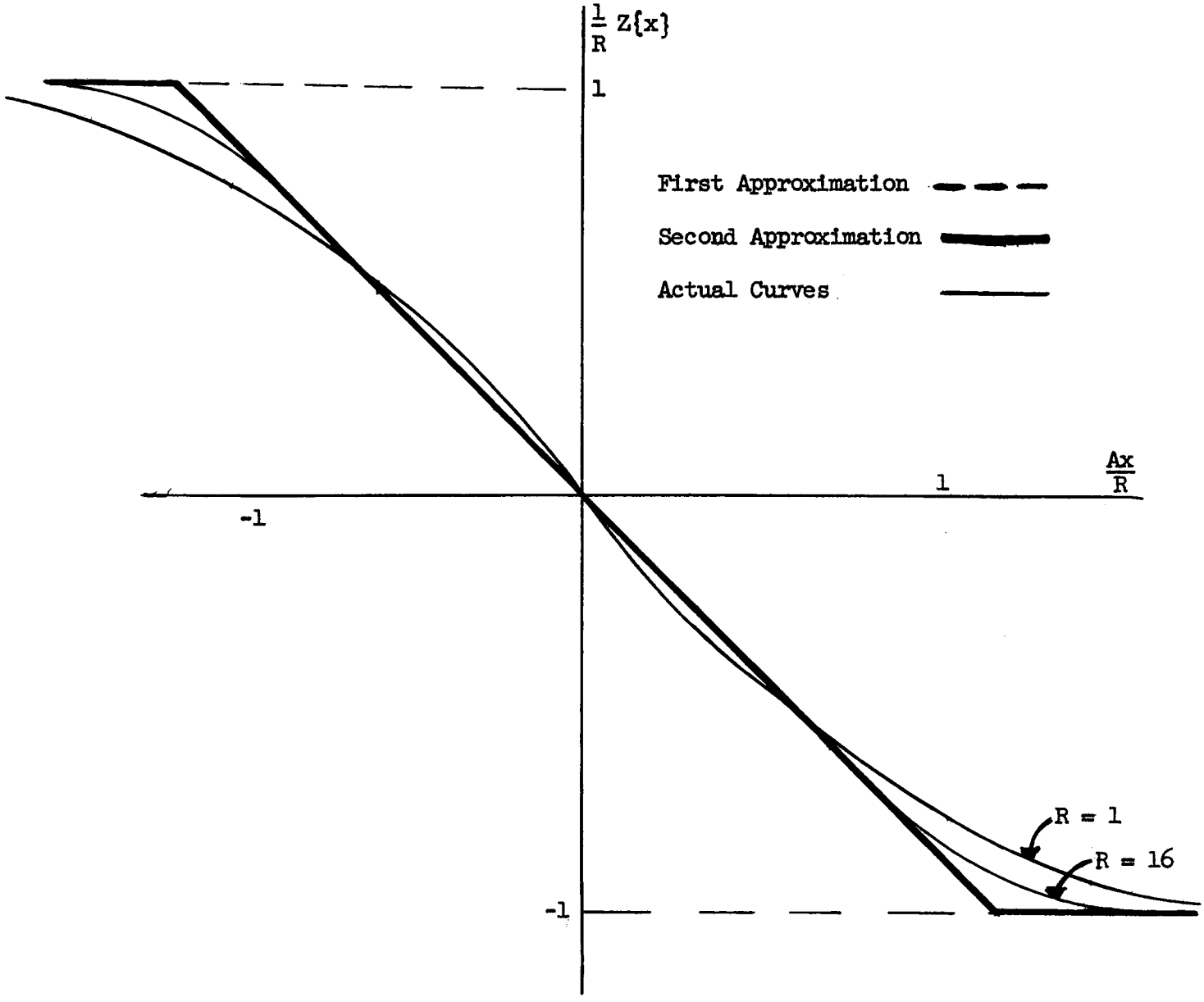

Fig. 5 Comparison of Approximations to Z{x}

4. Performance

The non-linearity of the ML decision statistic Λ_k, as given by (3), discourages an exact analytical determination of the per-symbol probability of error P_e. We will be content, therefore, to find upper and lower bounds for P_e.

A reasonable lower bound is easily established. If we want to plot P_e versus ρ, the signal-to-noise ratio, then we must choose r, the index of interference, as a parameter. Obviously, the most favorable condition is $r = 0$ which means that the main portion of the pulse s(t) is orthogonal to its tail. If such is the case, proper filtering can extract this tail and the particular time slot occupied by the tail is unimportant. We may consider that it is, in fact, sent during the same time slot as the main body of the pulse. Thus the total signal energy is available in one baud and we have the usual, interference-less probability of error given by $\mathrm{Erfc}\{\sqrt{\rho}\}$, where

$$\mathrm{Erfc}\{x\} \equiv \frac{1}{\sqrt{2\pi}} \int_x^\infty e^{-\frac{t^2}{2}}\, dt. \tag{11}$$

Our lower bound on P_e is, then,

$$\mathrm{Erfc}\{\sqrt{\rho}\} < P_e. \tag{12}$$

To establish the upper bound on P_e we establish the probability of error for a sub-optimum detector. To this end we separate A_k of Equation (1) into

$$A_k = c_k + d_k\ , \tag{13}$$

where

$$c_k \equiv \frac{4}{N_o} \int_{kT}^{(k+1)T} y(t)\, s(t-kT)\, dt \tag{14}$$

and

$$d_k \equiv \frac{4}{N_o} \int_{(k+1)T}^{(k+2)T} y(t)\, s(t-kT)\, dt. \tag{15}$$

Thus c_k is the correlation of the data with the first part of the pulse, $s(t)$, and d_k is the correlation of the data with the pulse's tail. With these definitions we can write the optimum statistic Λ_k of Equation (3) as

$$\Lambda_k = c_k + Z\{c_{k-1} + d_{k-1} + Z\{c_{k-2} + d_{k-2} + \cdots\}\}$$

$$+ d_k + Z\{d_{k+1} + c_{k+1} + Z\{d_{k+2} + c_{k+2} + \cdots\}\}.$$

Now we use the first approximation $Z'\{x\}$ to $Z\{x\}$ as given by Equation (9) to yield a new statistic

$$c_k - R\ \mathrm{Sgn}\{c_{k-1} + d_{k-1} - R\ \mathrm{Sgn}\{\cdots\}\}$$

$$+ d_k - R\ \mathrm{Sgn}\{d_{k+1} + c_{k+1} - R\ \mathrm{Sgn}\{\cdots\}\}.$$

The statistic to be studied, U_k, is then found by setting to zero all d terms under the first Sgn bracket and all c terms under the second. Thus

$$U_k = U_k^- + U_k^+, \tag{16}$$

where

$$U_k^- = c_k - R\ \mathrm{Sgn}\{U_{k-1}^-\} \tag{17}$$

and

$$U_k^+ = d_k - R\ \mathrm{Sgn}\{U_{k+1}^+\}. \tag{18}$$

Note that U_k^- is a "tail cancellation" detector* operating only on the data up to $(k+1)T$ and U_k^+ is its counterpart operating only on data after $(k+1)T$.

It can be shown** that if U_k^- is used as a decision statistic for μ_k it yields a probability of error P_e^- given by

$$P_e^- = \frac{\operatorname{Erfc}\left\{\sqrt{\frac{C}{2}}\right\}}{1 + \operatorname{Erfc}\left\{\sqrt{\frac{C}{2}}\right\} - \frac{1}{2}\operatorname{Erfc}\left\{\frac{C+2R}{\sqrt{2C}}\right\} - \frac{1}{2}\operatorname{Erfc}\left\{\frac{C-2R}{\sqrt{2C}}\right\}}, \tag{19}$$

where

$$C \equiv \frac{4}{N_o}\int_0^T s^2(t)\,dt. \tag{20}$$

Thus, we deduce that U_k^+ yields a probability of error

$$P_e^+ = \frac{\operatorname{Erfc}\left\{\sqrt{\frac{D}{2}}\right\}}{1 + \operatorname{Erfc}\left\{\sqrt{\frac{D}{2}}\right\} - \frac{1}{2}\operatorname{Erfc}\left\{\frac{D+2R}{\sqrt{2D}}\right\} - \frac{1}{2}\operatorname{Erfc}\left\{\frac{D-2R}{\sqrt{2D}}\right\}}, \tag{21}$$

where

$$D \equiv \frac{4}{N_o}\int_T^{2T} s^2(t)\,dt. \tag{22}$$

---

*U_k^- is exactly the switched mode detector of Reference (6).

**R. A. Gonsalves, unpublished notes for Course 3.906, Northeastern University, 1966; this may also be deduced from Reference (6).

With these definitions of C and D we can write U_k more explicitly as

$$U_k = \mu_k(C+D) + n_k + R(\mu_{k-1} + \mu_{k+1}) - R\{\text{Sgn } U_{k-1}^-\} - R\{\text{Sgn } U_{k+1}^+\}\ , \tag{23}$$

where

$$n_k \equiv \frac{4}{N_o} \int_{kT}^{(k+2)T} n(t)\ s(t-kT)\ dt. \tag{24}$$

The desired probability of error P_e^{+-} is

$$P_e^{+-} = P(U_k < 0 \,|\, \mu_k = 1)$$

or

$$P_e^{+-} = \frac{1}{4}\,[P_1 + P_2 + P_3 + P_4], \tag{25}$$

where

$$P_1 \equiv P(U_k < 0 \,|\, \mu_{k-1} = 1,\ \mu_k = 1,\ \mu_{k+1} = 1), \tag{26}$$

$$P_2 \equiv P(\mu_k < 0 \,|\, \mu_{k-1} = 1,\ \mu_k = 1,\ \mu_{k+1} = -1),$$

etc. We can evaluate these 4 probabilities, as the following evaluation of P_1 indicates.

From (23) and (26)

$$P_1 = P(C + D + n_k + 2R - R\ \text{Sgn}\{U_{k-1}^-\} - R\ \text{Sgn}\{U_{k+1}^+\} < 0 \,|\, \mu_{k-1} = 1,\ \mu_k = 1,\ \mu_{k+1} = 1). \tag{27}$$

But n_k is independent of both U_{k-1}^- and U_{k+1}^- since, from (24), n_k depends on the white noise from kT to (k+2)T while U_{k-1}^- considers data prior to kT and U_{k+1}^+ considers data after (k+2)T. Also, U_{k-1}^- and U_{k+1}^+, conditioned on $\mu_{k-1} = 1$, $\mu_k = 1$, and $\mu_{k+1} = 1$, are also independent. Thus P_1 expands into

$$P_1 = P(n_k < -C-D)\, P(U_{k-1}^- > 0 \,|\, \mu_{k-1}=1)\, P(U_{k+1}^+ > 0 \,|\, \mu_{k+1}=1)$$

$$+ P(n_k < -C-D-4R)\, P(U_{k-1}^- < 0 \,|\, \mu_{k-1}=1)\, P(U_{k+1}^+ < 0 \,|\, \mu_{k+1}=1)$$

$$+ P(n_k < -C-D-2R)\, P(U_{k-1}^- < 0 \,|\, \mu_{k-1}=1)\, P(U_{k+1}^+ > 0 \,|\, \mu_{k+1}=1)$$

$$+ P(n_k < -C-D-2R)\, P(U_{k-1}^- > 0 \,|\, \mu_{k-1}=1)\, P(U_{k+1}^+ < 0 \,|\, \mu_{k+1}=1)$$

$$= Q_e^+ Q_e^- \operatorname{Erfc}\left\{\sqrt{\frac{C+D}{2}}\right\} + P_e^+ P_e^- \operatorname{Erfc}\left\{\frac{C+D+4R}{\sqrt{2(C+D)}}\right\}$$

$$+ (Q_e^- P_e^+ + Q_e^+ P_e^-) \operatorname{Erfc}\left\{\frac{C+D+2R}{\sqrt{2(C+D)}}\right\},$$

where

$$Q_e^+ = 1 - P_e^+ ,$$

$$Q_e^- = 1 - P_e^- ,$$

since, from (24) n_k is Gaussian with mean zero and variance $2(C+D)$, and since $P(U_{k-1}^- > 0 \,|\, \mu_{k-1}=1)$ is exactly $Q_e^- = 1 - P_e^-$, etc.

In a similar fashion we can establish P_2, P_3 and P_4. The resulting P_e^{+-} is

$$P_e^{+-} = (Q^-Q^+ + \tfrac{1}{2} P^-P^+) \operatorname{Erfc}\left\{\sqrt{\frac{C+D}{2}}\right\}$$

$$+ \tfrac{1}{2} (Q^-P^+ + P^-Q^+) \left[\operatorname{Erfc}\left\{\frac{C+D+2R}{\sqrt{2(C+D)}}\right\} + \operatorname{Erfc}\left\{\frac{C+D-2R}{\sqrt{2(C+D)}}\right\}\right]$$

$$+ \tfrac{1}{4} (P^-P^+) \left[\operatorname{Erfc}\left\{\frac{C+D+4R}{\sqrt{2(C+D)}}\right\} + \operatorname{Erfc}\left\{\frac{C+D-4R}{\sqrt{2(C+D)}}\right\}\right]. \qquad (28)$$

This is our upper bound on P_e for the ML detector. Thus

$$\text{Erfc}\{\sqrt{\rho}\} < P_e < P_e^{+-} \quad . \tag{29}$$

In the derivation of the upper bound we were required to separate the main portion of the pulse from its tail. Thus, in order to plot P_e vs. ρ, we need a new parameter which defines the division of energy. Let

$$a \equiv \frac{D}{C} = \frac{\int_T^{2T} s^2(t)\, dt}{\int_0^T s^2(t)\, dt} \tag{30}$$

be the required parameter. Then Figures 6, 7, 8, and 9 for a = .25, .50, .75 and 1.0 show this upper bound, Equation (28), versus ρ for several values of r.

Since Schwartz's inequality requires

$$\left[\int_0^T s(t)\, s(t+T)\, dt\right]^2 \le \int_0^T s^2(t)\, dt \int_0^T s^2(t+T)\, dt$$

we have the following inequality for C, D, and R

$$R^2 \le CD.$$

This implies the inequality

$$|r| \le \frac{\sqrt{a}}{1+a} \tag{31}$$

and accounts for the choices of the parameter r in Figures 6, 7, 8, and 9. Finally, since P_e^{+-} is symmetric in R and since C and D can be interchanged, Figures 6 through 9 apply also for a = 4, 2, 1.33 and 1 respectively, and for r or -r, as indicated.

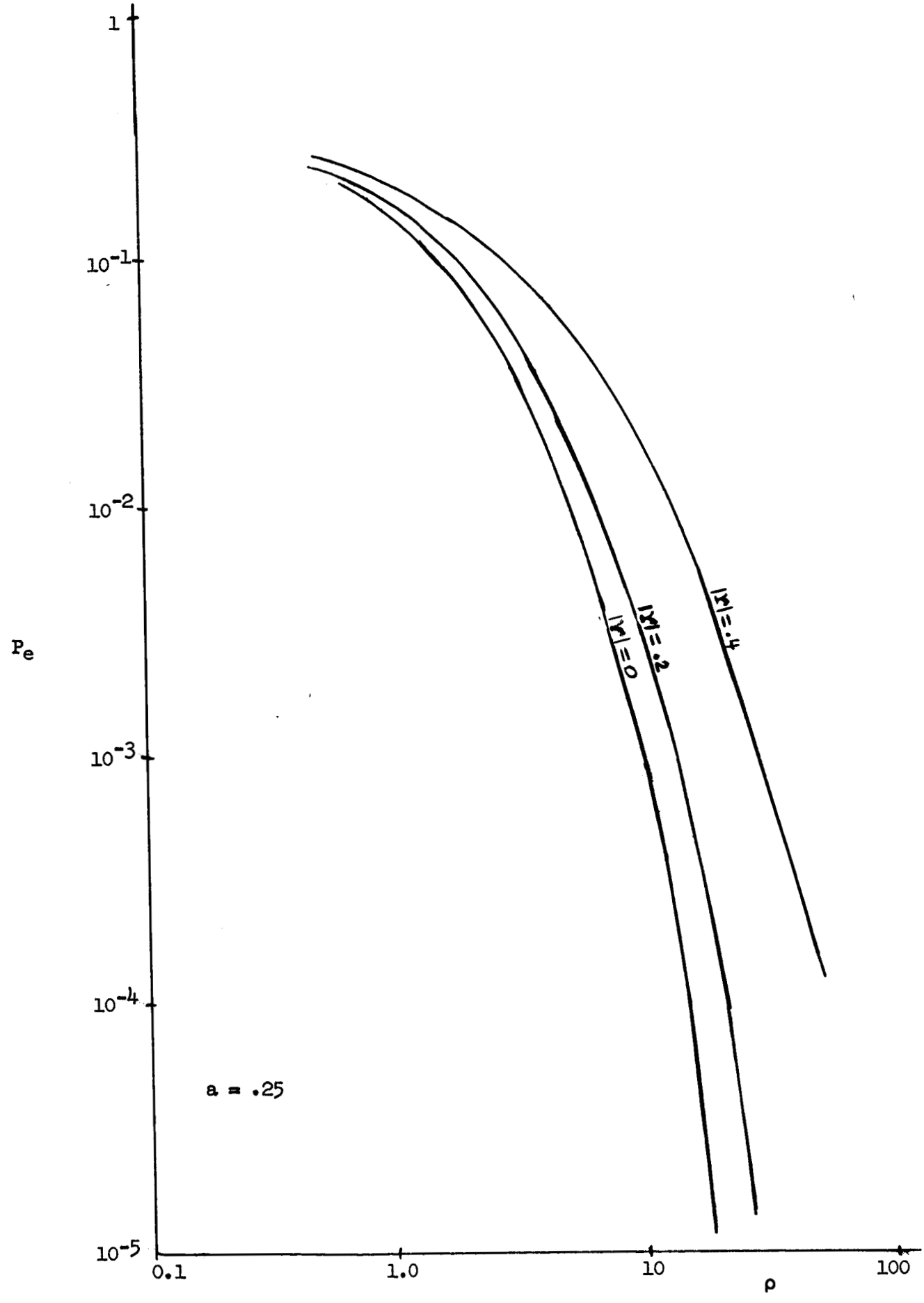

Fig. 6 P_e vs. ρ, a = .25, 4.0

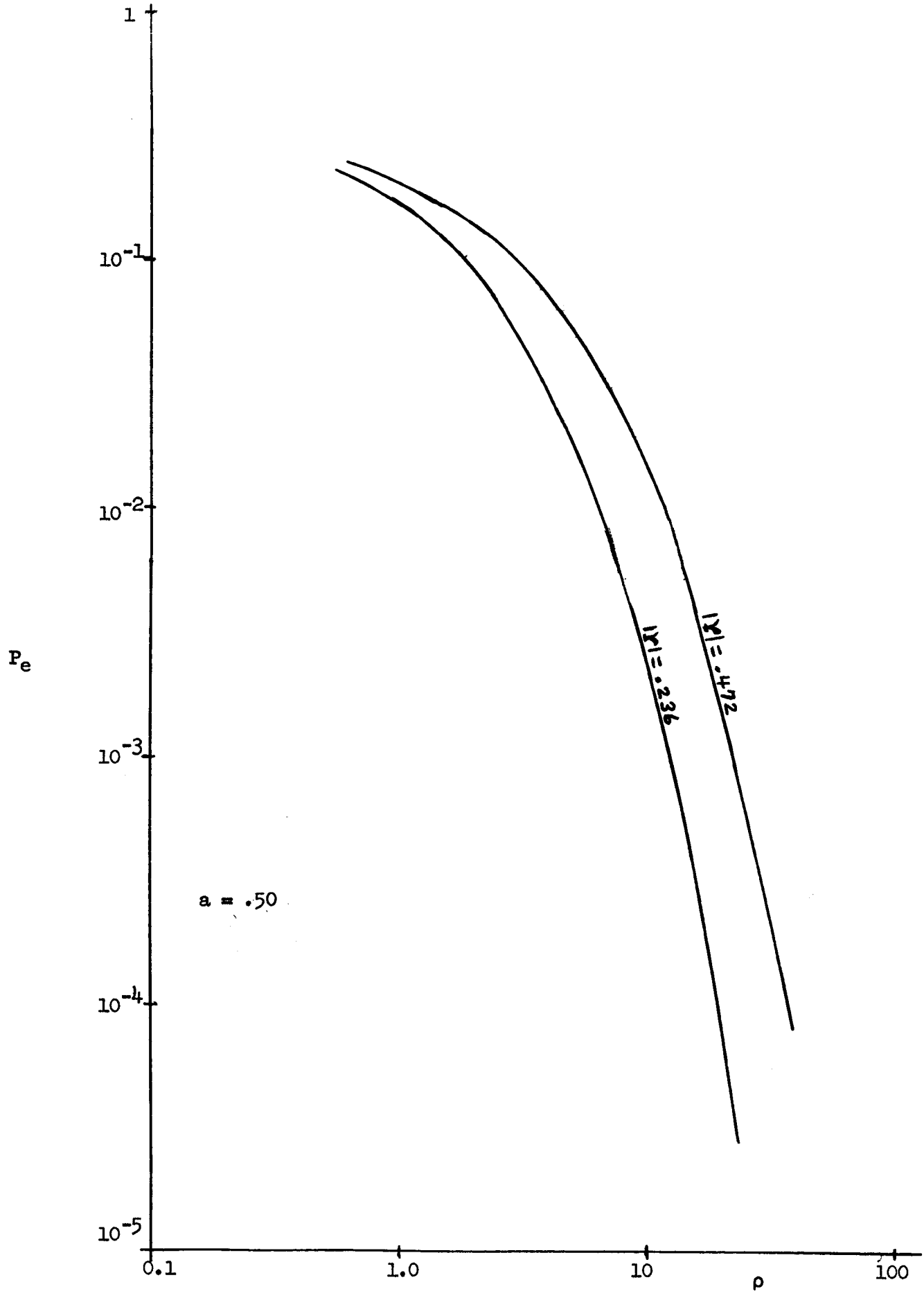

Fig. 7 P_e vs. ρ, a = .50, 2.0

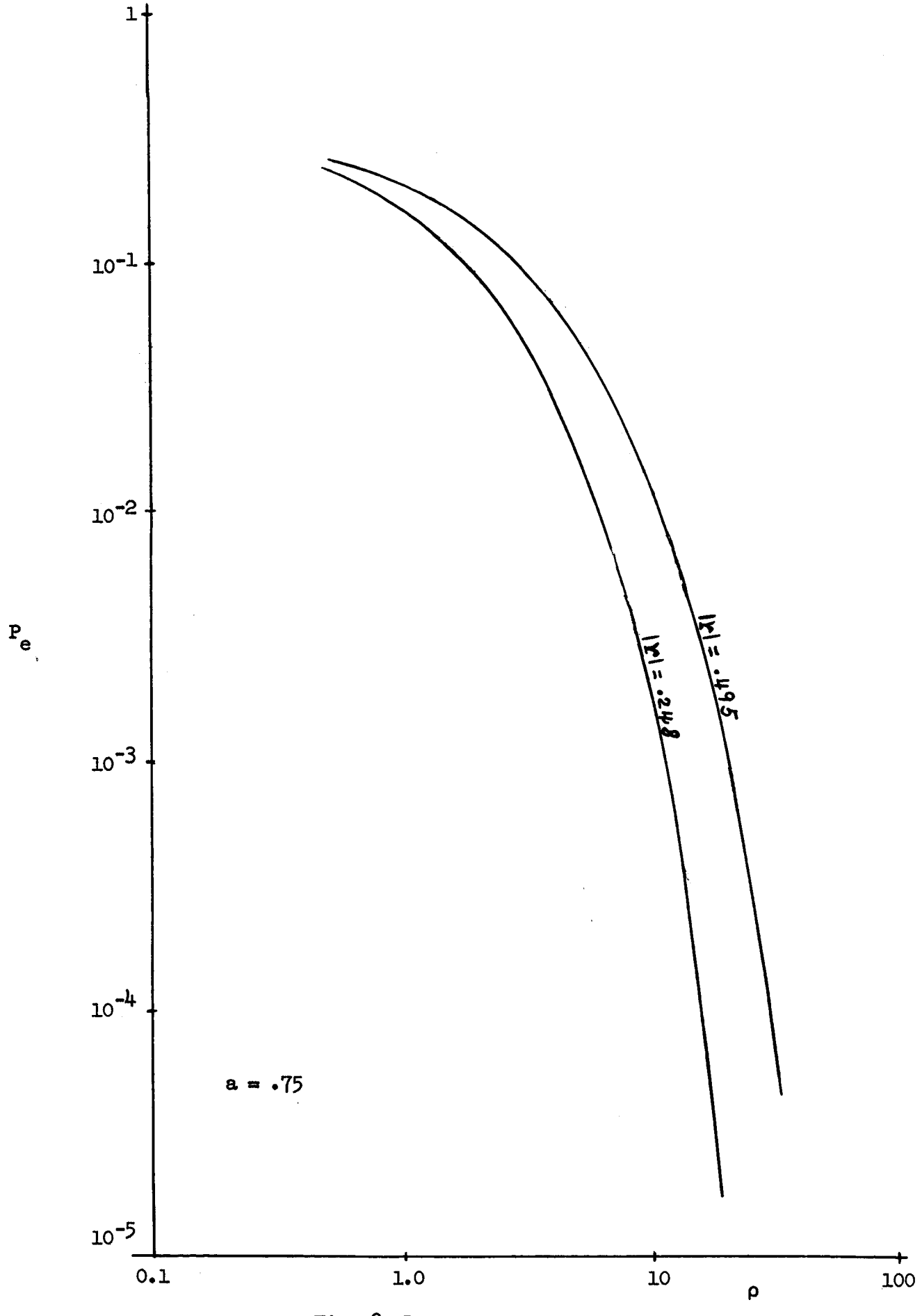

Fig. 8 P vs. ρ, a = .75 , 1.33

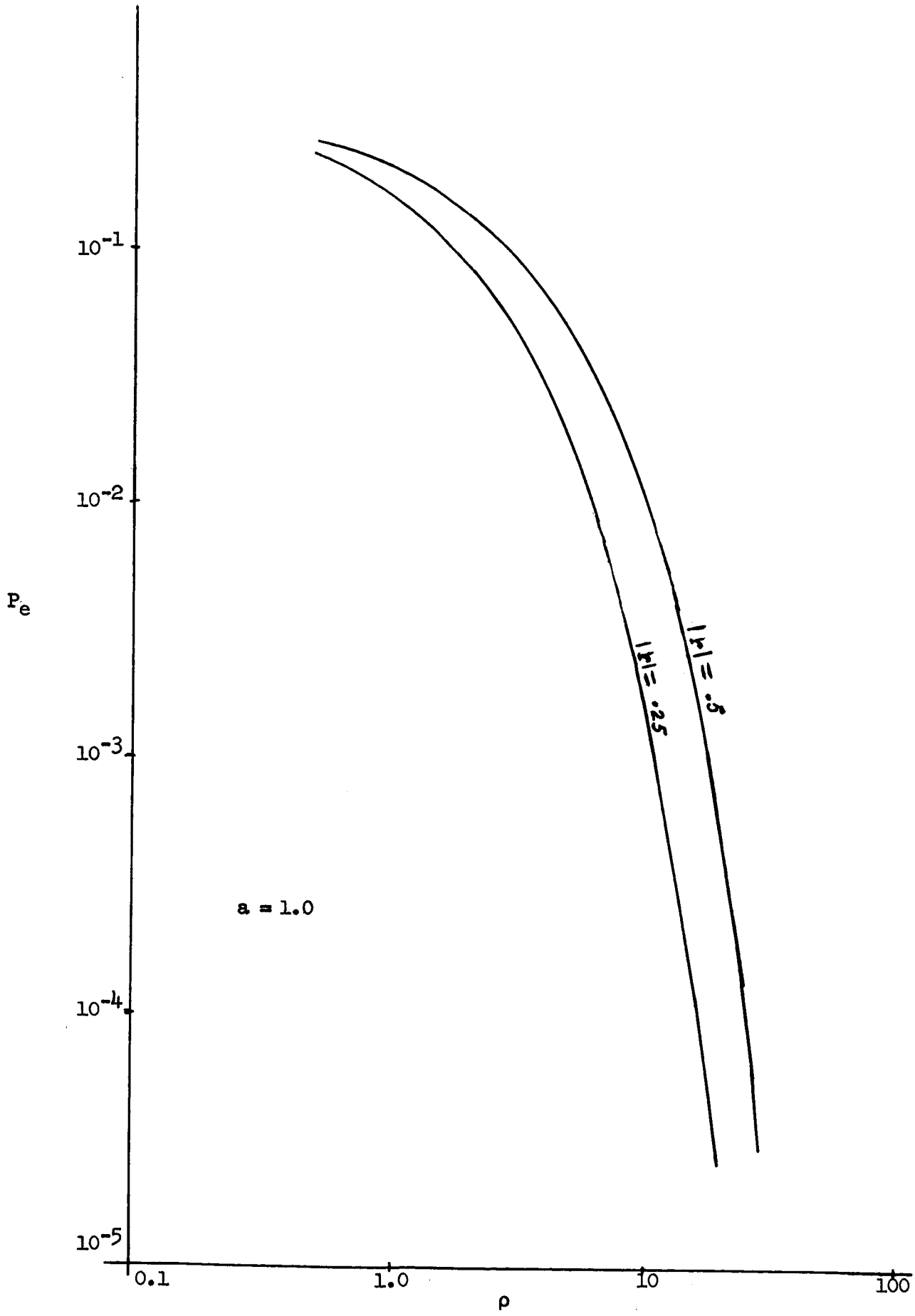

Fig. 9 P_e vs. ρ, a = 1.0

To compare the performance of the ML detector with others we assume the unit energy pulse s(t) as shown in Fig. 10. Since s(t) is symmetric about t = T, we have a = 1. Then the output, of the matched filter of Fig. 2 would be g(t) as shown, if s(t) alone were sent. This is, of course, the autocorrelation function $\phi_{ss}(t)$ of s(t) delayed by 2T seconds so the index of interference r is

$$r \equiv \frac{\int_0^{2T} s(t)\, s(t+T)\, dt}{\int_0^{T} s^2(t)\, dt} = \frac{g(T)}{g(2T)} = .25.$$

From the inequality (31) this is about one-half the maximum interference that can occur. In Fig. 11 we show the resulting upper and lower bounds on P_e for the ML detector. Also shown in this figure is the tail cancellation detector which operates only on the past data, with probability of error given by Equation (19).

In Reference [4], Fig. 5, Tufts and Aaron present a similar curve for the probability of error of an optimized linear detector. That curve is drawn for a symmetric pulse s(t), implying a = 1, and for r = 0.2. It is reproduced in Fig. 11 for comparison. We can see that the upper bound on P_e and this new curve nearly coincide. Since the upper bound is established by considering a detector which uses the tail cancellation principle for both past and future data, this indicates that such a detector is nearly equivalent to an optimum linear detector.

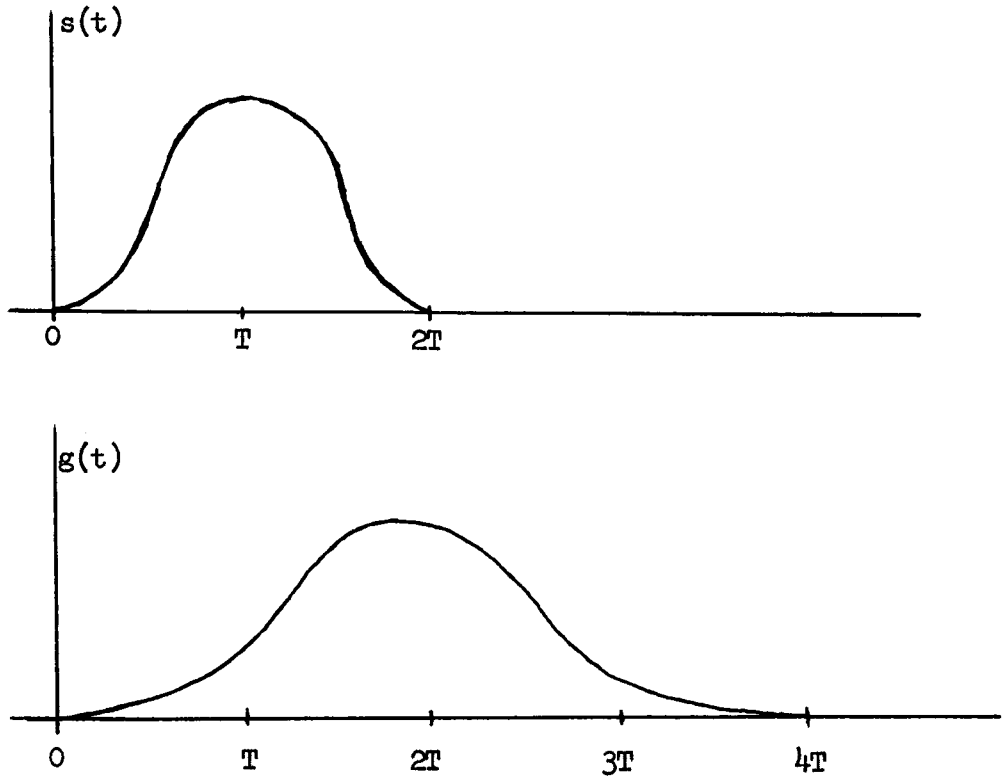

Fig. 10 Input Pulse and the Matched Filter Output

Finally, as discussed in the introduction, the ML detector will always yield a P_e smaller than that of a linear detector since the ML detector is not restricted by a constraint on linearity. Therefore, the "linear detector" curve of Fig. 11 actually serves as another upper bound on P_e.

5. Extensions

Consider the multi-level case where μ_k can take on one of M distinct values, $a_1, a_2, \ldots, a_M$. Then using a_1 as a reference, the ML detector computes

$$\Lambda_{ki} = \frac{P(\mu_k = a_i \,|\, \text{all data})}{P(\mu_k = a_1 \,|\, \text{all data})}, \quad i = 1,2,\ldots,M,$$

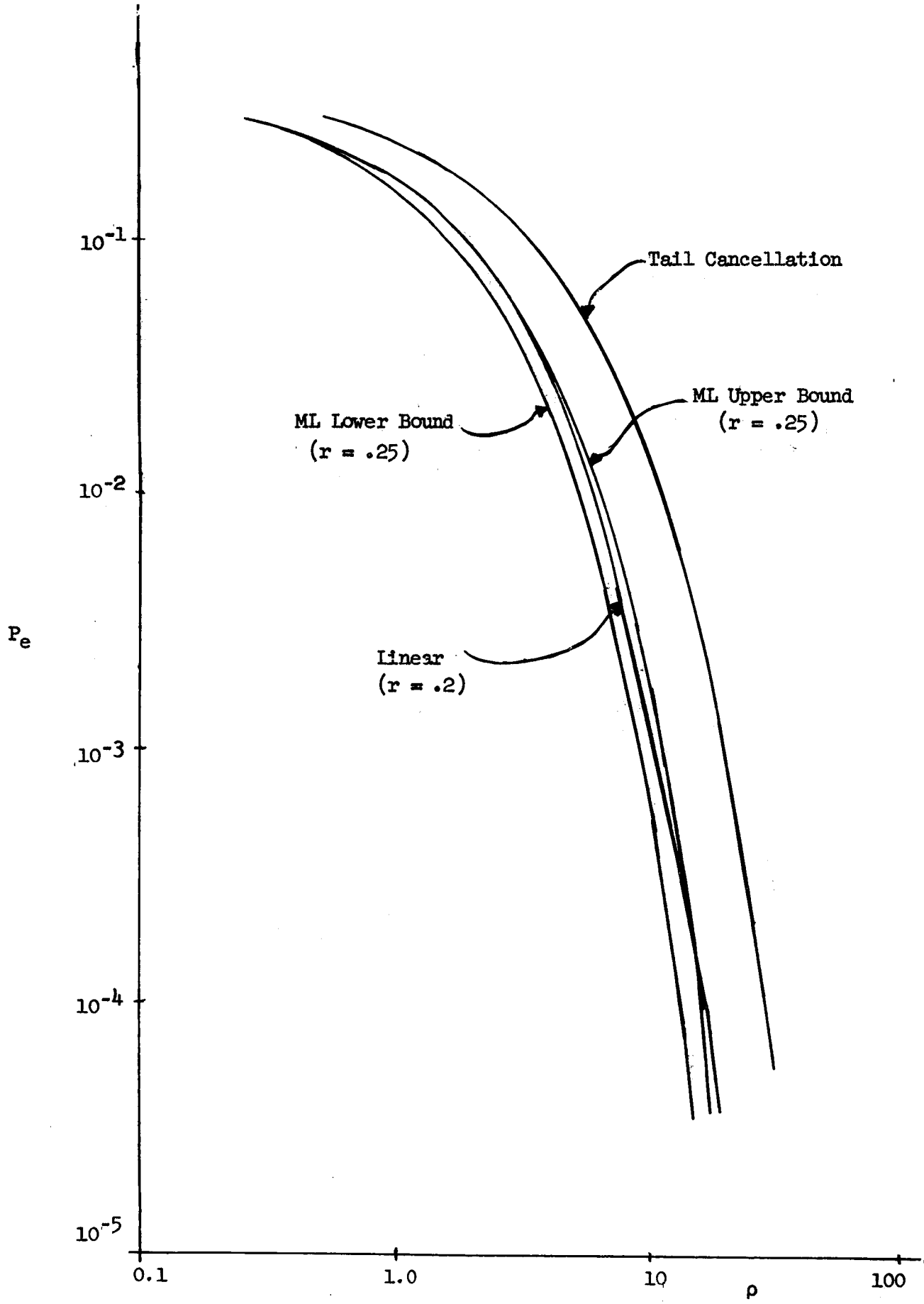

Fig. 11 Comparison of the ML, Tail Cancellation and Linear Receivers

and chooses that a_i which yields the largest Λ_{ki}. We can show that Λ_{ki} is given by

$$\Lambda_{ki} = (a_i - a_1) \frac{A_k}{2} + B_i(A_{k-1}, A_{k-2}, \ldots) + B_i(A_{k+1}, A_{k+2}, \ldots),$$

where A_k is the same A_k as that of Equation (1) and the B_i functions are similar to the previously encountered Z function, Equation (4). It appears that one could find an upper bound on the performance of this detector by a direct extension of the approach used in the binary case. A search for efficient implementation of this detector and the actual bounding of the P_e are recommended for further study.

The major limitation of the approach taken in this report is the assumption that intersymbol interference exists only between adjacent symbols. It is apparent that this restriction is met if the autocorrelation function $\phi_{ss}(\tau)$ of $s(t)$ is zero for $\tau = \pm 2T, \pm 3T, \ldots$. If such is the case, the signal can actually last for more than two bauds. The time function of Fig. 12 is an example of such an acceptable $s(t)$. In fact, we may interpret the restriction to mean that the autocorrelation function is non-zero only at $\tau = 0$ and at $\tau = \pm KT$, K an integer. Such might be the case when the interference is due to multipath, but only two paths are important. See Fig. 13. In implementing such a receiver the delay line tap spacings are simply changed from T seconds to KT seconds.

Finally we recommend for further study the form of the ML detector when the autocorrelation function is non zero at more than one integer multiple removed from $\tau = 0$. From the extension above, we hypothesize

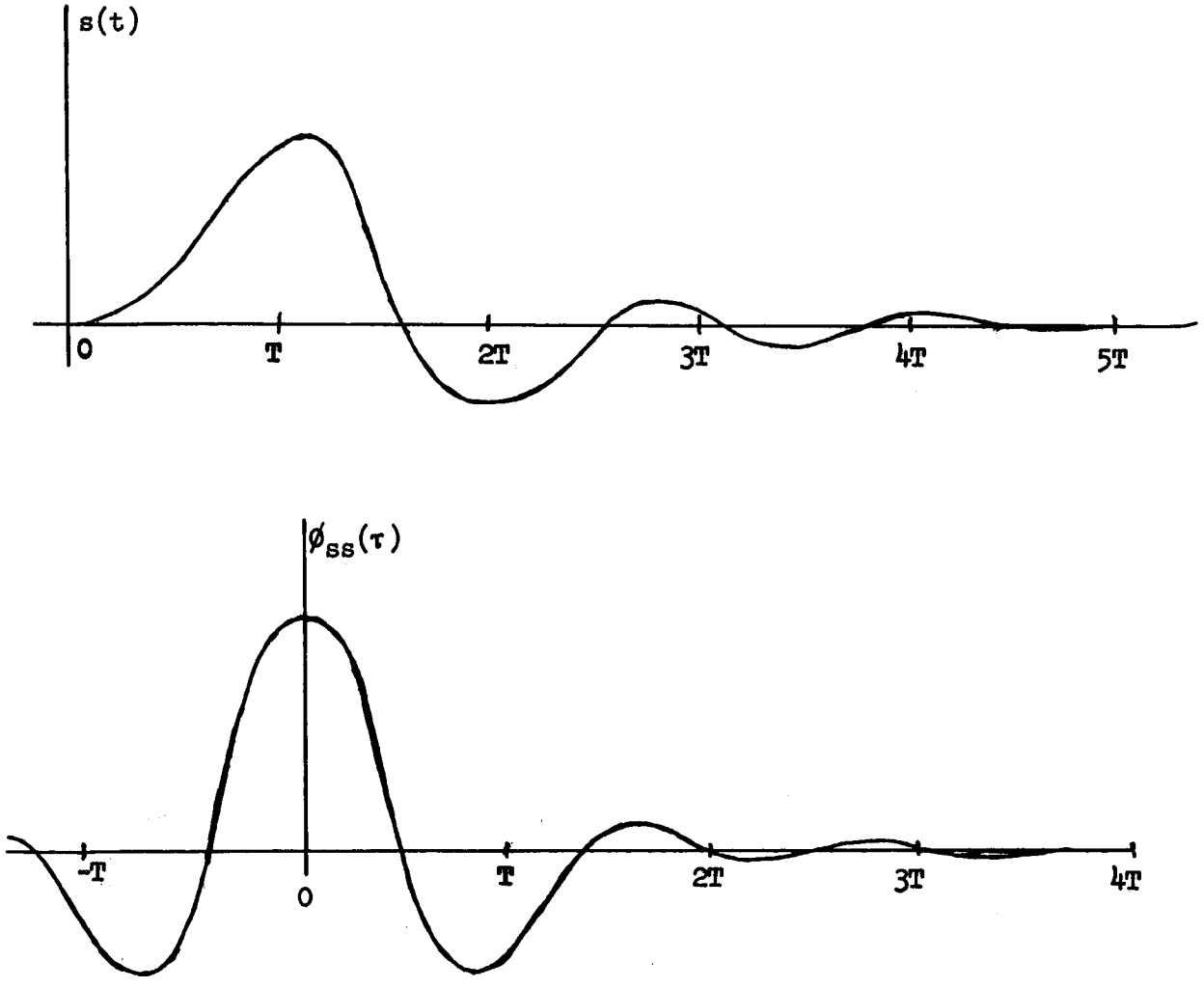

Fig. 12 Acceptable s(t)

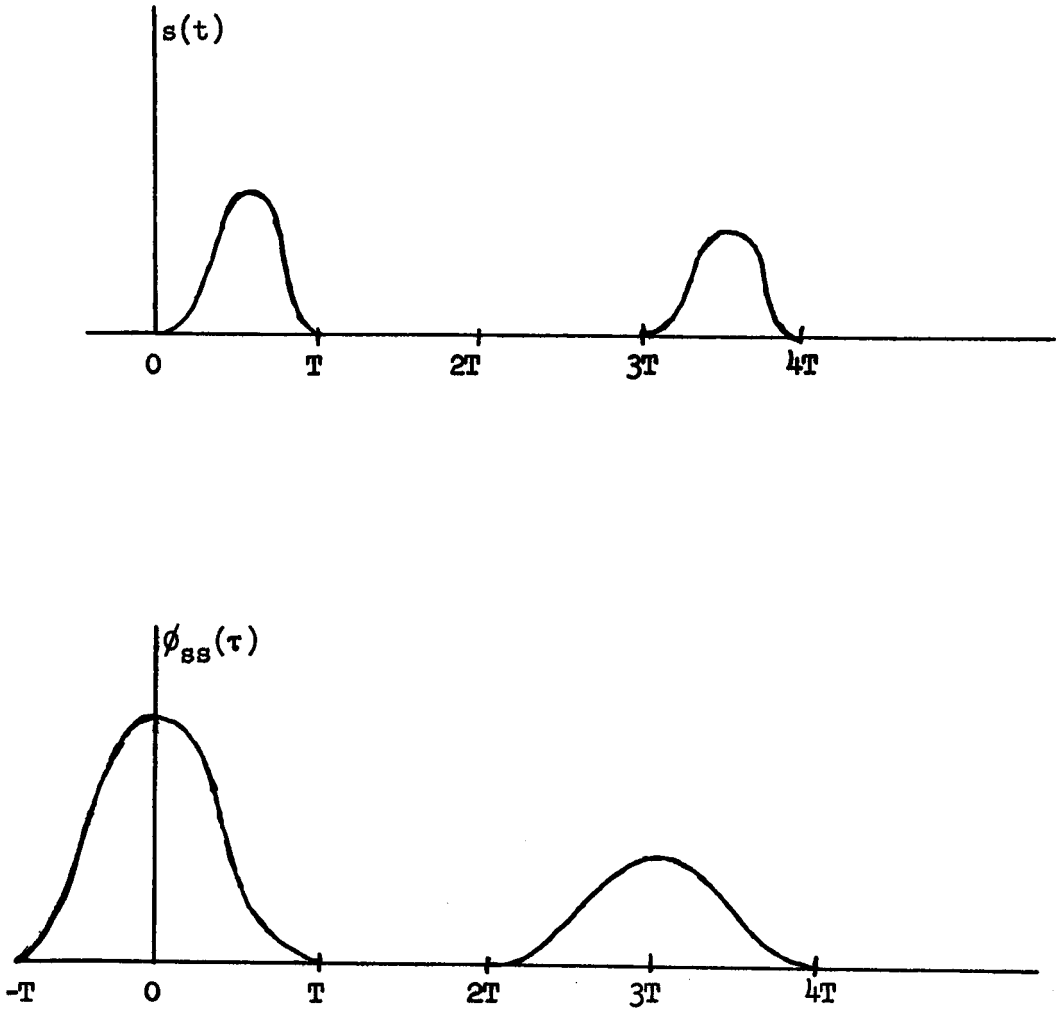

Fig. 13 Another Acceptable s(t)

that a good approximation to this detector, for interference between three symbols, will take the form of Fig. 14, where

$$Z_i\{x\} \equiv \frac{e^{x} + e^{R_i}}{1 + e^{x+R_i}} , \tag{32}$$

and

$$R_i \equiv \frac{4}{N_o} \int_{-\infty}^{\infty} s(t)\, s(t+iT)\, dt. \tag{33}$$

This detector structure is specified by three parameters, R_1, R_2 and R_3, and using the approximation $Z_i\{x\} \approx -R_i\ \mathrm{Sgn}\{x\}$ might be easily implemented and analyzed. In that figure

$$\Lambda_k = A_k + B_{k-1}^{-} + B_{k+1}^{+}$$

where $$B_k^{-} = A_k + Z_1\{B_{k-1}^{-}\} + Z_2\{B_{k-2}^{-} +\} \cdots$$

and $$B_k^{+} = A_k + Z_1\{B_{k+1}^{+}\} + Z_2\{B_{k+2}^{+}\} + \cdots \ .$$

6. Conclusions

Implementation of the ML detector when intersymbol interference exists only between adjacent symbols is fairly simple. The detector consists of a filter matched to the signal pulse s(t) followed by a tapped delay line and a feedback loop (Fig. 2). The detector strucutre, excluding the matched filter, is dependent on a single parameter R, given by $R = 2\rho r$, where ρ is the signal-to-noise ratio, Equation (7), and r is the index of interference, Equation (8). Thus the optimum detector structure can easily be adapted to a changing signal-to-noise ratio.

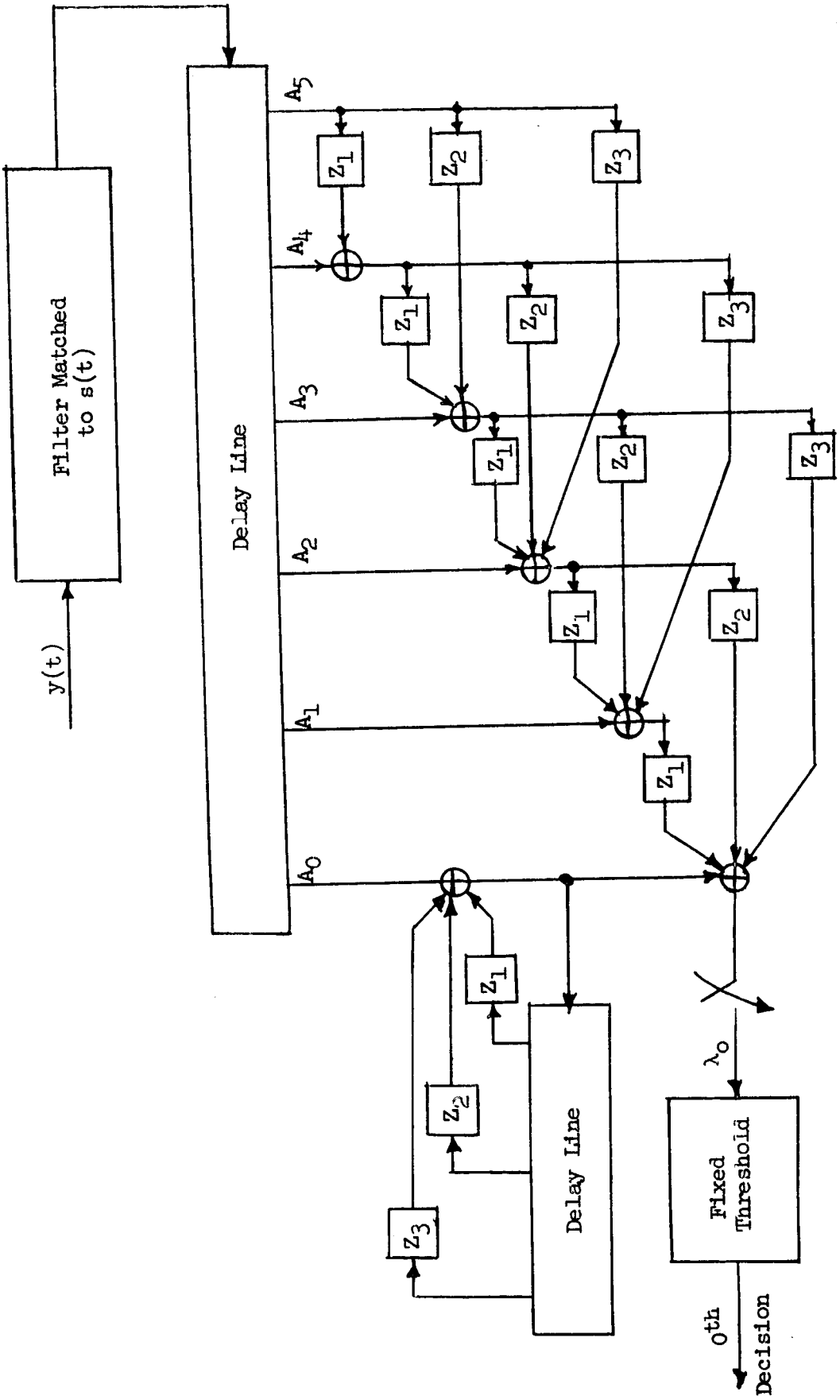

Fig. 14 Possible Detector Configuration for Extended ISI

The performance of the ML detector can be adequately bounded. These bounds are presented in Figures 6 through 9. A gross approximation to the ML detector, that which approximates $Z\{x\}$ the non-linear amplifier of Equation (4), by a saturating amplifier, as indicated in Equation (9), appears to perform as well as an optimum linear detector and may be easier to implement.

We indicate that these results can be extended to the multi-level case and suggest an approximation to the ML detector for significant interference between more than one symbol.

REFERENCES

1. R. A. Gonsalves and W. H. Lob, "Maximum-Likelihood Detection in a Binary Channel with Memory", Scientific Report No. 4, Northeastern University, AFCRL-63-313, July 1963.

2. J. M. Wozencraft and I. M. Jacobs, Principles of Communication Engineering, John Wiley & Sons, 1965, p. 489.

3. R. W. Lucky, "Automatic Equalization for Digital Communication", Bell System Technical Journal, April 1965.

4. M. R. Aaron and D. W. Tufts, "Intersymbol Interference and Error Probability", IEEE Transactions on Information Theory, January 1966.

5. D. W. Tufts, "Nyquist's Problem - The Joint Optimization of Transmitter and Receiver in Pulse Amplitude Modulation", Proceedings of the IEEE, March 1965.

6. J. M. Aein and J. C. Hancock, "Reducing the Effects of Intersymbol Interference with Correlation Receivers", IEEE Transactions on Information Theory, July 1963.

Unclassified

Security Classification

DOCUMENT CONTROL DATA - R&D

(Security classification of title, body of abstract and indexing annotation must be entered when the overall report is classified)

1. ORIGINATING ACTIVITY *(Corporate author)*
Northeastern University
360 Huntington Avenue
Boston, Massachusetts

2a. REPORT SECURITY CLASSIFICATION
Unclassified

2b. GROUP

3. REPORT TITLE
"Implementation and Performance of the Maximum-Likelihood Detector in a Channel with Intersymbol Interference

4. DESCRIPTIVE NOTES *(Type of report and inclusive dates)*
Scientific Interim Report

5. AUTHOR(S) *(Last name, first name, initial)*
Gonsalves, Robert A.

6. REPORT DATE	7a. TOTAL NO. OF PAGES	7b. NO. OF REFS
August 1966	39	6

8a. CONTRACT OR GRANT NO.	9a. ORIGINATOR'S REPORT NUMBER(S)
AF19(628)-3312 NASA Grant NGR-22-011-013	Scientific Report No. 5
b. PROJECT AND TASK NO. 4610-03	
c. DOD ELEMENT 62405304	9b. OTHER REPORT NO(S) *(Any other numbers that may be assigned this report)*
d. DOD SUBELEMENT 674610	AFCRL-66-586

10. AVAILABILITY/LIMITATION NOTICES
Distribution of this document is unlimited.

11. SUPPLEMENTARY NOTES	12. SPONSORING MILITARY ACTIVITY
National Aeronautics Space Administration	Hq., AFCRL, OAR (CRB) United States Air Force L. G. Hanscom Field, Bedford, Mass.

13. ABSTRACT

It is shown that the maximum-likelihood (ML) detector for noisy, binary channel with restricted intersymbol interference (ISI) consists of a matched filter followed by a tapped delay line. The useful output is a nonlinear function of the tap outputs. Bounds on the per-symbol probability of error indicate that a gross approximation to the ML detector performs as well as an optimum linear detector. The major assumptions are (1) bi-polar binary signals, (2) ISI only between adjacent bauds, (3) stationary additive white, Gaussian noise, and (4) perfect synchronization. Extensions are suggested to remove assumptions (1) and (2) and to handle stationary, non-white Gaussian noise.

DD FORM 1 JAN 64 1473

Unclassified

Security Classification

Unclassified

Security Classification

14. KEY WORDS	LINK A		LINK B		LINK C	
	ROLE	WT	ROLE	WT	ROLE	WT
Maximum-Likelihood Intersymbol Interference Matched Filter Non-Linear Detector Tapped Delay Line Probability of Error						

INSTRUCTIONS

1. ORIGINATING ACTIVITY: Enter the name and address of the contractor, subcontractor, grantee, Department of Defense activity or other organization *(corporate author)* issuing the report.

2*a*. REPORT SECURITY CLASSIFICATION: Enter the overall security classification of the report. Indicate whether "Restricted Data" is included. Marking is to be in accordance with appropriate security regulations.

2*b*. GROUP: Automatic downgrading is specified in DoD Directive 5200.10 and Armed Forces Industrial Manual. Enter the group number. Also, when applicable, show that optional markings have been used for Group 3 and Group 4 as authorized.

3. REPORT TITLE: Enter the complete report title in all capital letters. Titles in all cases should be unclassified. If a meaningful title cannot be selected without classification, show title classification in all capitals in parenthesis immediately following the title.

4. DESCRIPTIVE NOTES: If appropriate, enter the type of report, e.g., interim, progress, summary, annual, or final. Give the inclusive dates when a specific reporting period is covered.

5. AUTHOR(S): Enter the name(s) of author(s) as shown on or in the report. Enter last name, first name, middle initial. If military, show rank and branch of service. The name of the principal author is an absolute minimum requirement.

6. REPORT DATE: Enter the date of the report as day, month, year, or month, year. If more than one date appears on the report, use date of publication.

7*a*. TOTAL NUMBER OF PAGES: The total page count should follow normal pagination procedures, i.e., enter the number of pages containing information.

7*b*. NUMBER OF REFERENCES: Enter the total number of references cited in the report.

8*a*. CONTRACT OR GRANT NUMBER: If appropriate, enter the applicable number of the contract or grant under which the report was written.

8*b*, 8*c*, & 8*d*. PROJECT NUMBER: Enter the appropriate military department identification, such as project number, subproject number, system numbers, task number, etc.

9*a*. ORIGINATOR'S REPORT NUMBER(S): Enter the official report number by which the document will be identified and controlled by the originating activity. This number must be unique to this report.

9*b*. OTHER REPORT NUMBER(S): If the report has been assigned any other report numbers *(either by the originator or by the sponsor)*, also enter this number(s).

10. AVAILABILITY/LIMITATION NOTICES: Enter any limitations on further dissemination of the report, other than those imposed by security classification, using standard statements such as:

(1) "Qualified requesters may obtain copies of this report from DDC."

(2) "Foreign announcement and dissemination of this report by DDC is not authorized."

(3) "U. S. Government agencies may obtain copies of this report directly from DDC. Other qualified DDC users shall request through

_____."

(4) "U. S. military agencies may obtain copies of this report directly from DDC. Other qualified users shall request through

_____."

(5) "All distribution of this report is controlled. Qualified DDC users shall request through

_____."

If the report has been furnished to the Office of Technical Services, Department of Commerce, for sale to the public, indicate this fact and enter the price, if known.

11. SUPPLEMENTARY NOTES: Use for additional explanatory notes.

12. SPONSORING MILITARY ACTIVITY: Enter the name of the departmental project office or laboratory sponsoring *(paying for)* the research and development. Include address.

13. ABSTRACT: Enter an abstract giving a brief and factual summary of the document indicative of the report, even though it may also appear elsewhere in the body of the technical report. If additional space is required, a continuation sheet shall be attached.

It is highly desirable that the abstract of classified reports be unclassified. Each paragraph of the abstract shall end with an indication of the military security classification of the information in the paragraph, represented as *(TS), (S), (C), or (U).*

There is no limitation on the length of the abstract. However, the suggested length is from 150 to 225 words.

14. KEY WORDS: Key words are technically meaningful terms or short phrases that characterize a report and may be used as index entries for cataloging the report. Key words must be selected so that no security classification is required. Identifiers, such as equipment model designation, trade name, military project code name, geographic location, may be used as key words but will be followed by an indication of technical context. The assignment of links, rules, and weights is optional.

Distribution List

USASDRL (SIGRA/SL-NAC)
Fort Monmouth, New Jersey
ATTN: Mr. G. Balano

USASDRL (SIGRA/SLNAC)
Fort Monmouth, New Jersey
ATTN: Mr. J. Bartow

SIGNATRON, Incorporated
594 Marrett Road
Lexington, Massachusetts 02173
ATTN: Dr. Phillip A. Bello

SIGNATRON, Incorporated
Miller Building
594 Marrett Road
Lexington, Massachusetts
ATTN: Dr. Julian Bussgang

New York University
School of Engineering Science
Department of Electrical Engineering
University Heights
Bronx, New York 10453
ATTN: Dr. Robert F. Cotellessa

General Dynamics/Fort Worth
Chief Librarian
Post Office Box 748
Fort Worth, Texas 76101
ATTN: P. R. DeTonnancour

Northeastern University
Office of Research Administration
360 Huntington Avenue
Boston, Massachusetts 02115
ATTN: M. W. Essigmann

Polytechnic Institute of Brooklyn
Research Coordinator
333 Jay Street
Brooklyn, New York 11201
ATTN: Jerome Fox

Massachusetts Institute of Technology
Librarian, Lincoln Laboratory
Post Office Box 73
Lexington, Massachusetts
ATTN: Mary A. Granese

The Johns Hopkins University
School of Engineering Science
34th and Charles
Baltimore, Maryland 21218
ATTN: W. H. Huggins

The Rand Corporation
1700 Main Street
Santa Monica, California
ATTN: Dr. R. E. Kalaba

Michigan State University
Electrical Engineering Department
Engineering Building
East Lansing, Michigan
ATTN: Dr. W. Kilmer

U. S. Army Electronics R&D Laboratories
Commanding Officer SELRA/XC
Fort Monmouth, New Jersey 07703
ATTN: Mr. Mattes

Parke Mathematical Laboratories, Inc.
One River Road
Carlisle, Massachusetts 01741
ATTN: Dr. Nathan Grier Parke, III

Syracuse University
Syracuse, New York
ATTN: Professor F. Reza

RCA - Defense Electronic Products
Staff Engineer - Bldg. 10, Floor 7
Organization of Chief Tech. Admin.
Camden, New Jersey
ATTN: Mr. Harold J. Schrader

Bell Telephone Laboratories
1600 Osgood Street
North Andover, Massachusetts 01845
ATTN: David Shnidman

General Electric Company
Research Laboratory
Post Office Box 1088
Schenectady, New York 12301
ATTN: Dr. R. L. Shuey

Sylvania Electronic Systems
Applied Research Laboratory
40 Sylvan Road
Waltham, Massachusetts 02154
ATTN: Dr. Seymour Stein

Harvard University
199 Pierce Hall
Oxford Street
Cambridge, Massachusetts 02138
ATTN: Dr. D. W. Tuft

Litton Systems, Incorporated
335 Bear Hill Road
Waltham, Massachusetts 02154
ATTN: Dr. David Van Meter

Stanford Research Institute
333 Ravenswood Avenue
Menlo Park, California 94025
ATTN: W. R. Vincent

Director - AFOSR
Research Information Office
Washington, D. C.
ATTN: Dr. Harold Wooster

Philco Corporation
Plant No. 50
Systems Engineering
4700 Wissahickon Avenue
Philadelphia, Pennsylvania 19144
ATTN: S. Zebrowitz

AFCRL (CRW) Stop 30
L. G. Hanscom Field
Bedford, Massachusetts 01731

Autonetics, Division of North American Aviation, Inc.
3370 Miraloma Avenue - Bldg. 202
Anaheim, California 92803
ATTN: Main Tech. Library D/503-31

HRB Singer, Incorporated
1517 Science Avenue
State College, Pennsylvania

ITT Federal Laboratories
500 Washington Avenue
Nutley, New Jersey
ATTN: Technical Library

Massachusetts Institute of Technology
Engineering Library
Room 10-550
Cambridge, Massachusetts 02139

Motorola, Incorporated
Post Office Box 5409
Phoenix, Arizona 85010
ATTN: Technical Library

National Security Agency
Fort George G. Meade
Maryland
ATTN: Director C3/TDL

Office of Naval Research
Department of the Navy
Washington, D. C.
ATTN: Code 427 - Electronics Branch

RADC (EMCRS)
Griffiss Air Force Base, New York 13442

Rand Corporation
1700 Main Street
Santa Monica, California 90406
ATTN: Library

Sandia Corporation - Sandia Base
Post Office Box 5800
Albuquerque, New Mexico
ATTN: Classified Document Division

Space Technology Laboratories, Inc.
STL Technical Library
Document Acquisitions
Post Office Box 95001
Los Angeles, California

The University of Michigan
Institute of Science and Technology
Box 618
Ann Arbor, Michigan 48107
ATTN: Technical Documents Service

Hq., AFCRL, OAR (CRBK) Stop 30
L. G. Hanscom Field
Bedford, Massachusetts 01730

AFCRL (CRMXLR) Stop 29
L. G. Hanscom Field
Bedford, Massachusetts 01730
ATTN: Mrs. Cora Gibson

AFCRL (CRMXLR) Stop 29
L. G. Hanscom Field
Bedford, Massachusetts 01730

AFCRL (CRMXRD) Stop 30
L. G. Hanscom Field
Bedford, Massachusetts 01730

AFCRL (CRMXRA) Stop 39
L. G. Hanscom Field
Bedford, Massachusetts 01730

AFCRL (CRN) Stop 30
L. G. Hanscom Field
Bedford, Massachusetts 01730

AFCRL (CRTE) Stop 30
L. G. Hanscom Field
Bedford, Massachusetts 01730

AFCRL (CRTPM) Stop 30
L. G. Hanscom Field
Bedford, Massachusetts 01730

ADC
Operations Analysis Office
Ent. Air Force Base, Colorado

AEDC (ARO, Inc.)
Arnold Air Force Station
Tennessee 37389
ATTN: Library/Documents

AFETR
Technical Library-MU-135
Patrick Air Force Base, Florida 32925

AFIT (MCLI, Library)
Building 125 - Area B
Wright-Patterson Air Force Base, Ohio 45433

AFSC-STLO (RSTAL)
AF Unit Post Office
Los Angeles, California 90045

AFSC-STLO (RTSAB)
Waltham Federal Center
424 Trapelo Road
Waltham, Massachusetts 02154

AFSC-STLO (RTSAS)
452 Deguigne
Sunnyvale, California 94086

AFSC-STLO (RTSUM)
68 Albany Street
Cambridge, Massachusetts 02139

AFSWC
Technical Library
Kertland Air Force Base, New Mexico

Director, Air University Library
Maxwell Air Force Base, Alabama 36112
ATTN: AUL3T

APGC
(PGBPS-12)
Eglin Air Force Base, Florida 32542

Hq., AWSAE/SIPB
Scott Air Force Base, Illinois 62225

OAR (RRY)
1400 Wilson Boulevard
Arlington, Virginia 22209

RADC (EMTDL)
Griffiss Air Force Base, New York 13440
ATTN: Documents Library

RTD
Scientific Director
Bolling Air Force Base
Washington, D. C.

RTD (APX)
Wright-Patterson Air Force Base
Ohio 45433

RTD (AWX)
Wright-Patterson Air Force Base
Ohio 45433

RTD (FDX)
Wright-Patterson Air Force Base
Ohio 45433

Systems Engineering Group (RTD)
Wright-Patterson Air Force Base
Ohio 45433
ATTN: SEPIR

SAC (OAI)
Offutt Air Force Base
Nebraska 68113

SSD (SSTRT)
Los Angeles Air Force Station
AFUPO
Los Angeles, California 90045
ATTN: Lt. O'Brien

Hq., TAC (OA)
Langley Air Force Base
Virginia 23362

USAF Academy
Academy Library (DFSLB)
Colorado 80840

USAF Academy
FJSRL
Colorado 80840

Hq., USAFSS (OSA)
San Antonio, Texas 78241

Army Electronic Proving Ground
Technical Library
Fort Huachuca, Arizona

Army Missile Command
Redstone Scientific Information Center
Redstone Arsenal, Alabama 35809
ATTN: Chief, Document Section

U. S. Army Research Office
3045 Columbia Pike
Arlington, Virginia 2204
ATTN: Technical Library

Los Alamos Scientific Laboratories
Los Alamos, New Mexico

U. S. Army Electronics Command
Technical Document Center
Fort Monmouth, New Jersey 07703
ATTN: AMSEL-RD-MAT

Bureau of Naval Weapons
(DLI - 31 - Library)
Washington, D. C.

Chief of Naval Operations
(OP-413-B21)
Washington, D. C.

Director
Naval Research Laboratory
Washington, D. C. 20390
ATTN: 2027

Naval Air Development Center
Library
Johnsville, Pennsylvania

Naval Missile Center
Library
Point Mugu, California

Naval Ordnance Laboratory
Technical Library
White Oak, Silver Spring
Maryland

U. S. Naval Postgraduate School
Library (Code 2124)
Monterey, California 93940

Commanding Officer and Director
U. S. Navy Electronics Laboratory
(Library)
San Diego, California 92152

Commander (Code 753)
U. S. Naval Ordnance Test Station
China Lake, California 93555
ATTN: Technical Library

Commanding Officer
Office of Naval Research Branch Office
Box 39 - Fleet Post Office
New York 09510

U. S. Naval Academy
Library
Annapolis, Maryland

ARPA
Library
The Pentagon
Washington, D. C.

Central Intelligence Agency
Washington, D. C. 20505
ATTN: OCR/DD/STD. Distribution

Director
Defense Atomic Support Agency
Washington, D. C. 20301
ATTN: Technical Library Section

Defense Documentation Center (DDC)
Cameron Station
Alexandria, Virginia 22314

DIA
(DIAAP-142)
Washington, D. C. 20301

FAA
Bureau of Research and Development
300 Independence Avenue, S.W.
Washington, D. C. 20553

Government Printing Office
Library
Division of Public Documents
Washington, D. C.

Library of Congress
Aerospace Technical Division
Washington, D. C. 20540

Library of Congress
Exchange and Gift Division
Washington, D. C. 20540

NAS/NRC - Library
Executive Secretary
Advisory Committee to AFSC
2101 Constitution Avenue, N.W.
Washington, D. C. 20418

NASA Scientific and Technical
Information Facility
Post Office Box 33
College Park, Maryland 20740
ATTN: Acquisitions Branch (S-AK/DL)

NASA - Ames Research Center
Technical Library
Moffett Field, California

Environmental Sciences Services Adm.
Library
Boulder Laboratories
Boulder, Colorado 80302

NSF
1951 Constitution Avenue, N.W.
Washington, D. C. 20235

ODDR+E (Library)
Room 3C-128
The Pentagon
Washington, D. C. 20301

Smithsonian Astrophysical Observatory -
Library
60 Garden Street
Cambridge, Massachusetts 02138

U. S. Atomic Energy Commission
Hq., Library - Room G-017
Reports Section
Washington, D. C. 20545

U. S. Weather Bureau
Library - ESSA - Room 806
8060 13th Street
Silver Spring, Maryland 20910

AIAA - Library
Technical Information Service
750 Third Avenue
New York, New York

Aerospace Corporation
Post Office Box 95085
Los Angeles, California 90045
ATTN: Library Acquisitions Group

NASA - Flight Research Center
Library
P. O. Box 273
Edwards, California 93523

NASA - Goddard Institute for Space Studies
(Library)
2880 Broadway
New York, New York 10025

NASA - Goddard Space Flight Center
Technical Library
Greenbelt, Maryland

NASA - Jet Propulsion Laboratory
4800 Oak Grove Drive
Pasadena, California 91103
ATTN: Library (TDS)

NASA - Langley Research Center
Technical Library
Langley Station
Hampton, Virginia

NASA - Lewis Research Center
Library - Mail Stop 60-3
21000 Brookpark Road
Cleveland, Ohio 44135

NASA - Manned Spacecraft Center
Technical Library
Houston, Texas 77058

Battelle Memorial Institute
Library
505 King Avenue
Columbus, Ohio 43201

Boeing Aero-Space Division
Post Office Box 3707
Seattle, Washington
ATTN: Dr. N. L. Krisberg

The Mitre Corporation
Post Office Box 208
Bedford, Massachusetts 01700
ATTN: Library

National Center for Atmospheric Research
NCAR Library, Acquisitions
Boulder, Colorado 80302

The Rand Corporation
1700 Main Street
Santa Monica, California 90406
ATTN: Library-D

TRW Systems
Director, Physical Research Center
One Space Park
Redondo Beach, California 90278
ATTN: David B. Langmuir

The Johns Hopkins University
2500 West & Rogers Avenue
Baltimore, Maryland 21215
ATTN: Dr. Carl Kaplan

IIT Research Institute
Document Library
10 West 35th Street
Chicago, Illinois 60616

Massachusetts Institute of Technology
Meteorology Department 54-1712
Cambridge, Massachusetts 02139
ATTN: Professor Henry G. Houghton

Rockefeller Institute
New York, New York
ATTN: Dr. Mark Kac

University of California
Department of Physics
Los Angeles, California
ATTN: Dr. Joseph Kaplan

University of Illinois
Department of Physics
Urbana, Illinois
ATTN: Prof. Frederick Seitz

British Defence Staffs
British Embassy
Scientifc Information Officer
3100 Massachusetts Avenue, N.W.
Washington, D. C. 20008

Chief, Canadian Defence
Research Staff
2450 Massachusetts Avenue, N.W.
Washington, D. C. 20008
(Technical and Scientific Reports
will be released for military purposes
only and any proprietary rights which
may be involved are protected by
United States/United Kingdon and
Canadian Government Agreements)

National Research Council
Library
Ottawa 2, Ontario
Canada

Distribution List for NASA, ERC

ERC - Library
NASA, ERC
575 Technology Square
Cambridge, Massachusetts 02139

NASA, ERC
Systems Research Laboratory
Guidance and Control Branch
575 Technology Square
Cambridge, Massachusetts 02139
ATTN: Mr. Stephen J. O'Neil

NASA, ERC
Systems Research Laboratory
Guidance and Control Branch
575 Technology Square
Cambridge, Massachusetts 02139
ATTN: Mr. Jean Roy